AGU PUBLICATIONS

Geophysical Research Letters

RESEARCH LETTER
10.1002/2013GL058836

Key Points:
- First application of backprojection for tracking changing volcanic tremor
- Array deconvolution needed to resolve kilometer-scale changes in tremor location
- Tremor imaging reveals escalation due to a shift toward an intracaldera lake

Supporting Information:
- Readme
- Figure S1
- Figure S2
- Figure S3
- Figure S4
- Figure S5
- Figure S6
- Figure S7
- Text S1
- Animation S1

Correspondence to:
M. M. Haney,
mhaney@usgs.gov

Citation:
Haney, M. M. (2014), Backprojection of volcanic tremor, *Geophys. Res. Lett.*, *41*, 1923–1928, doi:10.1002/2013GL058836.

Received 25 NOV 2013
Accepted 24 JAN 2014
Accepted article online 28 JAN 2014
Published online 19 MAR 2014

Backprojection of volcanic tremor

Matthew M. Haney[1]

[1] Alaska Volcano Observatory, U. S. Geological Survey Volcano Science Center, Anchorage, Alaska, USA

Abstract Backprojection has become a powerful tool for imaging the rupture process of global earthquakes. We demonstrate the ability of backprojection to illuminate and track volcanic sources as well. We apply the method to the seismic network from Okmok Volcano, Alaska, at the time of an escalation in tremor during the 2008 eruption. Although we are able to focus the wavefield close to the location of the active cone, the network array response lacks sufficient resolution to reveal kilometer-scale changes in tremor location. By deconvolving the response in successive backprojection images, we enhance resolution and find that the tremor source moved toward an intracaldera lake prior to its escalation. The increased tremor therefore resulted from magma-water interaction, in agreement with the overall phreatomagmatic character of the eruption. Imaging of eruption tremor shows that time reversal methods, such as backprojection, can provide new insights into the temporal evolution of volcanic sources.

1. Introduction

Time reversal is a fundamental property inherent to all wave phenomena [*Fink*, 1997]. Seismic waves are no exception, and time reversal can be exploited for the purposes of imaging sources and structures in the Earth. With the installation of vast new seismic networks, the use of time reversal in source seismology has become widespread following the demonstration of the backprojection technique for the 2004 Sumatra-Andaman earthquake [*Ishii et al.*, 2005]. Backprojection has subsequently proved to be indispensable for understanding the time-dependent rupture of global earthquakes [*Walker and Shearer*, 2009]. The process has in fact become automated, and backprojection images are now computed and posted in near real time after large earthquakes by the Incorporated Research Institutions for Seismology Data Management Center [*Trabant et al.*, 2012].

Lokmer et al. [2009] and *O'Brien et al.* [2011] showed that such uses of time reversal have implications for the field of volcano seismology. At volcanoes, seismic signals are often characterized by emergent onsets, a lack of clear phase arrivals, and long durations. As such, they defy conventional location techniques. The difficulty in locating these types of volcanic events is troubling given that they are direct manifestations of fluid flow and magma migration within active volcanoes. Volcanic tremor, in particular, is a ubiquitous type of eruption seismicity [*McNutt and Nishimura*, 2008] that remains poorly understood. *Lokmer et al.* [2009] utilized numerical simulations to show that time reversal techniques are suitable for locating synthetic volcanic tremor signals given a dense enough local seismic network. By time-reversing recorded waveforms at Mount Etna, *O'Brien et al.* [2011] located a discrete long-period (LP) event. The time reversal studies by *Lokmer et al.* [2009] and *O'Brien et al.* [2011] differ from backprojection in that the backpropagation step is performed by a full waveform modeling code instead of waveform summation over surfaces of constant traveltime, or isochrons, as in *Ishii et al.* [2005]. The radial semblance method of *Almendros and Chouet* [2003] employs such an isochron summation to locate very long period (VLP) events at Kilauea Volcano and therefore bears similarities to backprojection.

Here we show the first application of backprojection for tracking a volcanic source whose location changes in time. We apply backprojection to VLP tremor at Okmok Volcano, Alaska, during its 2008 eruption and are able to detect kilometer-scale changes in tremor location. The spatial resolution is made possible by deconvolving the array response function from successive backprojection images. The movement of the tremor source is notable since it occurred during the hour leading up to an increase in tremor amplitude. The deconvolved images indicate that the main source of tremor generation shifted toward an intracaldera lake and that the subsequent tremor escalation resulted from the interaction of magma and water, i.e., hydrovol-

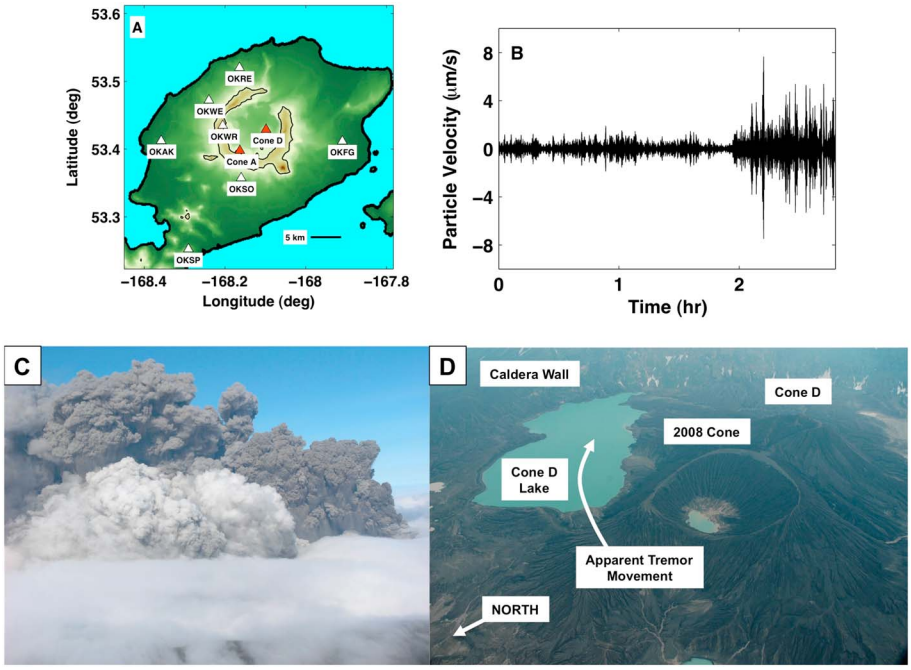

Figure 1. (a) Map of Okmok caldera, operational seismic stations during the 2008 eruption, and intracaldera cones discussed in text. (b) Seismogram from station OKSO beginning at 10:00 UTC on 2 August 2008 and band passed between 0.2 and 0.3 Hz. The tremor amplitude increased substantially at approximately 12:00 UTC, causing AVO to raise the aviation color code to red. (c) View toward the west on 2 August 2008 showing both an ash and a steam plume (Janet Schaefer, AVO/ADGGS). (d) View toward the southeast on 19 August 2010 (Jessica Larsen, AVO/UAF-GI). The change in tremor location observed from the backprojection results corresponds to an apparent movement toward the caldera wall and the intracaldera lake known as Cone D lake.

canism. These results demonstrate that backprojection and time reversal methods can track the evolution of seismic sources at the volcano scale.

2. Data

The 2008 Okmok eruption produced significant volcanic seismicity for over a month, from 12 July until 23 August 2008. The local network at Okmok during the 2008 eruption consisted of seven stations (Figure 1a), including two broadband three-component instruments (Guralp 6-TDs) and five short-period single-component instruments (Marks Products L4s). The network is maintained by the Alaska Volcano Observatory (AVO), a partnership between the University of Alaska Fairbanks Geophysical Institute (UAF-GI), the Alaska Division of Geological and Geophysical Surveys (ADGGS), and the U.S. Geological Survey. We apply instrument corrections to the raw data to obtain particle velocity seismograms and as a result remove the effect of different types of instruments within the network. Although the L4 short-period seismometers have a corner frequency of 1 Hz, they are capable of recording frequencies down to 0.1 Hz [*Haney et al.*, 2012]. Recent historical eruptions of Okmok have occurred at Cone A, an intracaldera cone located in the southwest portion of the caldera (Figure 1a). The 2008 eruption departed from the recent historical record [*Larsen et al.*, 2009] by building a new cone located to the north of an intracaldera cone known as Cone D (Figure 1a).

We analyze the eruption tremor during different hour-long periods on 23 July and 2 August. In the following sections, we discuss the 23 July tremor first since it has been previously analyzed by *Haney* [2010] and was continuous and stable in character. It therefore provides a test example prior to the analysis of the 2 August tremor, which underwent a strong escalation at 12:00 UTC and caused AVO to raise the aviation color code to red [*Larsen et al.*, 2009]. The 2 August episode was remarkable since the aviation code was raised to red based on the increase in seismicity; however, no large ash plumes were detected in subsequent satellite images.

3. Methods

We focus on the eruption tremor around a center frequency of 0.25 Hz, which is unusually low for eruption tremor [*McNutt and Nishimura*, 2008]. Although unusual in its frequency content, *Haney* [2010] found that the Okmok tremor was dominated by surface waves as is normally the case for eruption tremor [*McNutt and Nishimura*, 2008]. The low-frequency content of the tremor, with signal in the VLP range [*Haney*, 2010], makes it ideal for backprojection. At these low frequencies and over the distances of the Okmok seismic network, *Haney* [2010] found that to a high degree of accuracy, surface wave propagation occurred in an effective laterally homogeneous medium. *Haney* [2010] exploited these properties to locate typical tremor observed during the 2008 Okmok eruption using a station-pair double-difference method [*Zhang et al.*, 2010]. That method is capable of locating tremor from a single source but is unable to locate tremor from multiple sources since it associates a single interstation traveltime with each station pair. For the case of multiple sources, a more general method such as backprojection is necessary.

In our implementation of backprojection, we search over a 2-D grid of image or output points, time shift the vertical component recordings over a certain time window according to an assumed Rayleigh wave velocity and candidate source location, and compute the stack power. The theoretical array response for a single source at frequency ω_0 evaluated at the output point $\vec{r}_o$ is described by the following equation:

$$p(\vec{r}_o, \omega_0) = \frac{1}{N_r} + \frac{2}{N_r^2} \sum_{i=1}^{N_r-1} \sum_{j=i+1}^{N_r} \cos\left(\omega_0[(\tau_{s,i} - \tau_{o,i}) - (\tau_{s,j} - \tau_{o,j})]\right) \tag{1}$$

where N_r is the number of receivers or stations, $\tau_{s,i}$ is the traveltime between the source and the ith receiver, $\tau_{o,i}$ is the traveltime between the output point and the ith receiver, $\tau_{s,j}$ is the traveltime between the source and the jth receiver, and $\tau_{o,j}$ is the traveltime between the output point and the jth receiver (see the supporting information for derivation).

Considering N_s candidate sources each radiating with an amplitude of m_k ($k = 1 : N_s$) and recorded by an array of N_r receivers, the theoretical stacked power is given by

$$p(\vec{r}_o, \omega_0) = \frac{1}{N_r} \sum_{k=1}^{N_s} \tilde{m}_k^2 + \frac{2}{N_r^2} \sum_{i=1}^{N_r-1} \sum_{j=i+1}^{N_r} \sum_{k=1}^{N_s} \tilde{m}_k^2 \cos\left(\omega_0[(\tau_{k,i} - \tau_{o,i}) - (\tau_{k,j} - \tau_{o,j})]\right) \tag{2}$$

where $\tilde{m}_k^2 = m_k^2 / \sum_{k=1}^{N_s} m_k^2$ is the relative power of the kth source. Equation (2) leads to a linear matrix-vector relation between the array stack and the relative power of the N_s sources

$$\vec{p} = \mathbf{G}\vec{m} \tag{3}$$

where $\mathbf{G}$ is a matrix of the theoretical array responses over the region under consideration, $\vec{m}$ is the relative power of the candidate sources, and $\vec{p}$ is the stacked power at the output points, i.e., the backprojection result. Equation (3) is an inverse problem that we solve with positivity constraints on $\vec{m}$ with the nonnegative least squares algorithm of *Lawson and Hanson* [1974] in order to deconvolve the array response function from the backprojection result. The positivity constraints are needed since $\vec{m}$, the relative source power, is a positive quantity. This problem could alternatively be solved by the Richardson-Lucy algorithm [*Richardson*, 1972; *Lucy*, 1974] as first pointed out for beamforming in a seismic context by *Nishida et al.* [2008]. The Richardson-Lucy algorithm also ensures positivity. To our knowledge, deconvolution of the array response function has not previously been discussed for backprojection, as it has been for beamforming [*Nishida et al.*, 2008].

4. Observations

Before discussing the characteristics of the Okmok tremor during the escalation on 2 August, we present the results for 1 h of tremor on 23 July. This is intended as a test case of the backprojection method since the 23 July tremor was stable and radiated from a single well-defined location north of Cone D [*Haney*, 2010]. Shown in Figure 2 are the backprojection results. For the analysis, we used a 24 km by 24 km regular grid of output points spaced every 600 m and centered on the caldera; thus, the image consists of 41 by 41 pixels. The backprojection considered candidate source locations on the same grid resulting in $N_s = 41^2 = 1681$. We segmented the hour-long continuous recordings at the N_r = seven stations in nonoverlapping 2 min

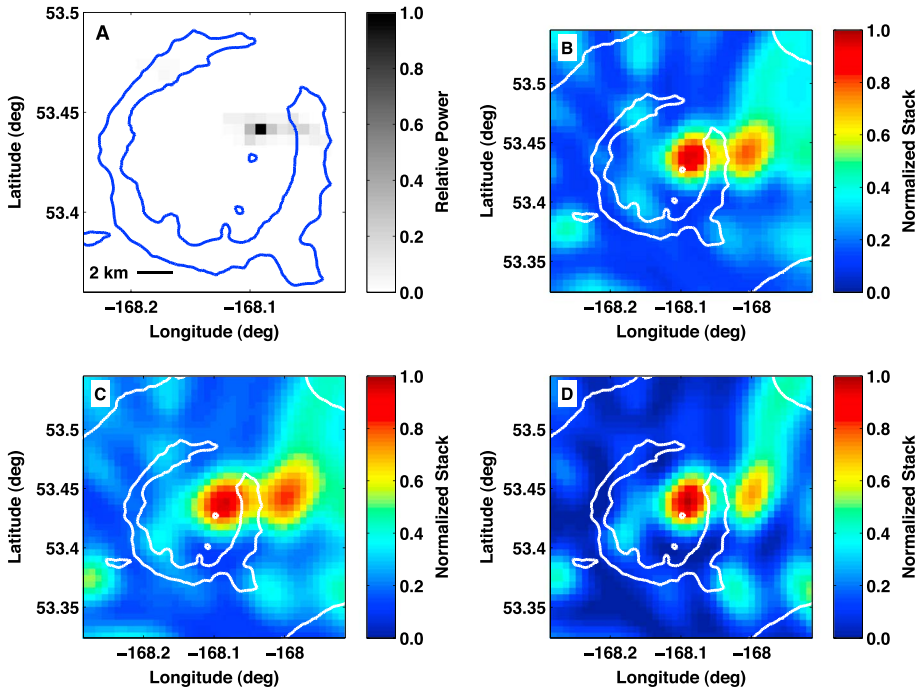

Figure 2. (a) Distribution of relative radiated power for typical tremor on 23 July 2008, computed by deconvolving the array response of the local network. (b) Backprojection result for 23 July tremor averaged over an hour. (c) Predicted backprojection result for 23 July tremor based on the tremor power distribution shown in Figure 2a. (d) Theoretical array response for a single tremor source to the north of Cone D. Significant blurring of the array response is due to the limited network at Okmok, in particular the secondary maximum outside of the caldera to the east.

time windows, band pass filtered the seismograms around 0.25 Hz using a cascade of third-order high-pass and low-pass Butterworth filters at 0.2 and 0.3 Hz, backprojected, and then summed each 2 min long backprojection over the entire hour to obtain an hour-long average backprojection. The array response was then deconvolved from the average backprojection to yield the final result. For computation of the traveltimes in equation (2), we assumed a laterally homogeneous Rayleigh wave velocity of 2.7 km/s at a frequency of 0.25 Hz as in *Haney* [2010].

The deconvolved backprojection in Figure 2a agrees with the previous findings of *Haney* [2010] since the tremor is observed to have originated in large part from a single location north of Cone D. Note the use of two additional stations (OKAK and OKSP in Figure 1a) that were not used in *Haney* [2010], which leads to a slight change in absolute location compared to *Haney* [2010]. Figure 2b shows the raw backprojection result for the entire hour. Owing to the modest size ($N_r = 7$) of the network at Okmok, the raw backprojection is significantly blurred, with a secondary maximum occurring outside of the caldera to the east. However, as depicted in Figure 2c, the synthetic backprojection obtained by applying equation (3) to the source power distribution in Figure 2a is able to reproduce the major features of the raw backprojection image in Figure 2b. The relative root-mean-square misfit over the entire domain is less than 5%. The impact of the limited network geometry can be appreciated from Figure 2d, which shows the theoretical impulse response from equation (1) for a single source north of Cone D.

We turn to the 2 August tremor and the tracking of an evolving source with backprojection. We analyze the 2 August tremor during two individual hour-long time periods, from 0 to 1 and 1 to2 h (10:00–11:00 and 11:00–12:00 UTC) as shown in Figure 1b. The second hour-long time period, from 1 to 2 h, immediately precedes the escalation in tremor that caused AVO to raise the aviation code to red at Okmok. Unfortunately, backprojection cannot be applied to the period of high-amplitude tremor after 2 h since the amplitudes saturated the five short-period seismometers at Okmok. Such saturation, or clipping, is known to damage the frequency domain properties of the signal, and as a result, band-pass filtering of the signals in the frequency band around 0.25 Hz is not possible. However, we demonstrate through backprojection that the tremor source had already begun changing in advance of the escalation, during the hour leading up to it.

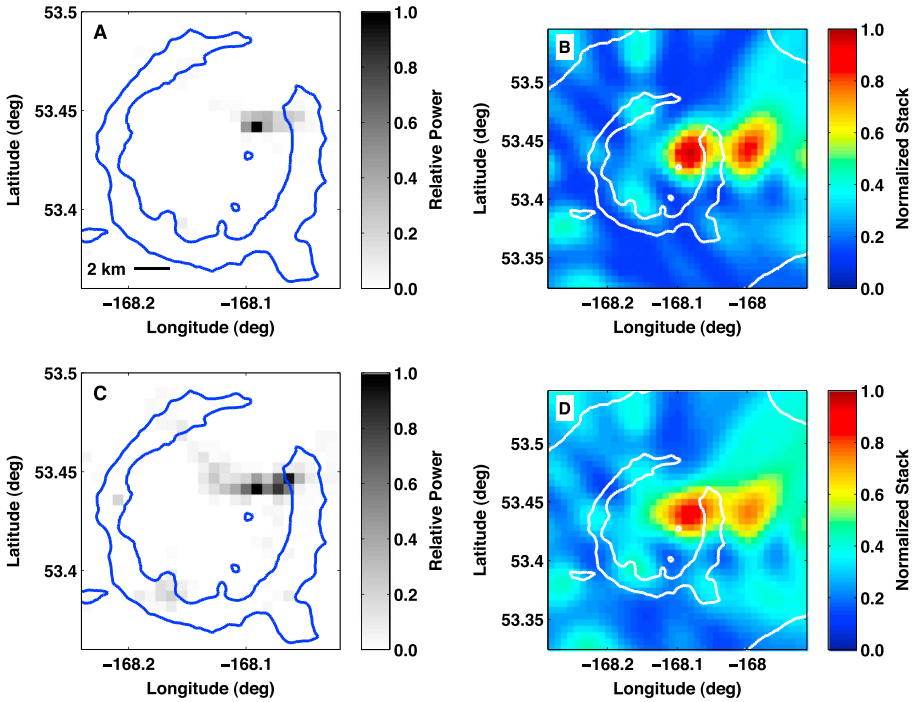

Figure 3. (a) Distribution of relative radiated power for tremor on 2 August 2008 during the time period from 0 to 1 h shown in Figure 1b, computed by deconvolution of the array response. (b) Backprojection result for 2 August tremor averaged over the time period from 0 to 1 h. (c) Distribution of relative radiated power for tremor on 2 August 2008 during the time period from 1 to 2 h shown in Figure 1b, again computed by deconvolution. (d) Backprojection result for 2 August tremor averaged over the time period from 1 to 2 h.

Deconvolved and raw backprojection images are plotted in Figure 3 for the time period from 0 to 1 h (Figures 3a and 3b, respectively) and 1 to 2 h (Figures 3c and 3d). The results from 0 to 1 h are similar to the 23 July tremor previously discussed in Figure 2. The tremor is dominated by the contribution from a single location to the north of Cone D. Backprojection over the time period from 1 to 2 h shows a different situation developed over the course of the hour prior to the tremor escalation. In addition to the tremor source active from 0 to 1 h, located to the north of Cone D, the source distribution in Figure 3c includes new locations to the northeast of Cone D, close to the wall of the caldera (see the supporting information for animation). Due to blurring, this apparent movement of the tremor source cannot be resolved in the raw backprojection result in Figure 3d. In this case, it would be incorrect to associate a single dominant source with the peak of the backprojection image. Instead, multiple sources active between 1 and 2 h interfere with each other in the backprojection image. This emphasizes the need for deconvolution of the array response from the backprojection image when working with the limited network at Okmok.

5. Discussion

The changes observed from 1 to 2 h suggest that the new sources near the caldera wall grew more powerful after 2 h and became the dominant source of the elevated tremor, overwhelming the typical tremor source to the north of Cone D. The apparent movement of the tremor toward the caldera wall (Figure 1d) is significant given the activity of the Okmok eruption on 2 August and the hydrology of the caldera. Figure 1c consists of a photograph taken approximately 8 h after the tremor escalation. To the northeast of Cone D lies an intracaldera lake known as Cone D lake (Figure 1d) that abuts the caldera wall. The new tremor sources imaged during the time period from 1 to 2 h in Figure 3d coincide spatially with the location of the lake, suggesting that the higher-amplitude tremor resulted from intense magma-water interaction. Field observations by AVO scientists on 2 August indicate that Cone D lake was drastically reduced in area approximately 8 h after the tremor escalation, with a shoreline modified relative to its normal position and sediments previously below the lake level exposed (T. Neal, written communication, 2013). Independent evidence for multiple tremor sources on 2 August at Okmok comes from the photograph in Figure 1c (view is toward the

west from the caldera rim), which shows simultaneous and distinct steam and ash plumes. The steam plume in the foreground of the photograph is to the east of the ash plume, consistent with it originating from the area near Cone D lake.

The field observations and photographic evidence, when taken together with the backprojection results, indicate that magma-water interaction at Cone D lake caused the tremor escalation on 2 August 2008. Interestingly, the high-amplitude tremor at 12:00 UTC was not correlated with a high-altitude ash plume; this agrees with the overall lack in correlation between tremor amplitude and ash plume height for the Okmok eruption after 1 August 2008 as noted by *Larsen et al.* [2009]. An explanation for the lack of ash production is that Cone D lake may have experienced boiling and drainage without coming into direct contact with magma during the tremor episode.

We have demonstrated the tracking of volcanic tremor arising from a temporally changing source with a novel backprojection method. Sufficiently high spatial resolution, necessary to discern kilometer-scale movement of the tremor source, is achieved through deconvolution of the network array response from the backprojection images. Location of volcanic tremor is an outstanding problem in volcano seismology, and backprojection techniques hold the promise of tracking this complex and poorly understood type of seismicity. These results open up new ways of observing volcanic processes, such as magma-water interaction, and motivate the increased use of time reversal methods to study volcanoes.

Acknowledgments

Stephanie Prejean (USGS-AVO), Tina Neal (USGS-AVO), Phil Dawson (USGS), and two reviewers are thanked for comments on this work. Any use of trade, firm, or product names is for descriptive purposes only and does not imply endorsement by the U.S. Government.

The Editor thanks Richard Aster and an anonymous reviewer for their assistance in evaluating this paper.

References

Almendros, J., and B. Chouet (2003), Performance of the radial semblance method for the location of very long period volcanic signals, *Bull. Seismol. Soc. Am.*, *93*, 1890–1903.

Fink, M. (1997), Time-reversed acoustics, *Phys. Today*, *50*, 34–40.

Haney, M. M. (2010), Location and mechanism of very long period tremor during the 2008 eruption of Okmok Volcano from interstation arrival times, *J. Geophys. Res.*, *115*, B00B05, doi:10.1029/2010JB007440.

Haney, M. M., J. Power, M. West, and P. Michaels (2012), Causal instrument corrections for short-period and broadband seismometers, *Seismol. Res. Lett.*, *83*(5), 834–845.

Ishii, M., P. M. Shearer, H. Houston, and J. E. Vidale (2005), Extent, duration and speed of the 2004 Sumatra–Andaman earthquake imaged by the Hi-Net array, *Nature*, *435*, 933–936.

Larsen, J., C. Neal, P. Webley, J. Freymueller, M. Haney, S. McNutt, D. Schneider, S. Prejean, J. Schaefer, and R. Wessels (2009), Eruption of Alaska volcano breaks historic pattern, *EOS, Trans. AGU*, *90*, 173–174.

Lawson, C. L., and R. J. Hanson (1974), *Solving Least Squares Problems*, Prentice-Hall, Englewood Cliffs, N. J.

Lokmer, I., G. S. O'Brien, D. Stich, and C. J. Bean (2009), Time reversal imaging of synthetic volcanic tremor sources, *Geophys. Res. Lett.*, *36*, L12308, doi:10.1029/2009GL038178.

Lucy, L. B. (1974), An iterative technique for the rectification of observed distributions, *Astron. J.*, *79*, 745–754.

McNutt, S. R., and T. Nishimura (2008), Volcanic tremor during eruptions: Temporal characteristics, scaling and constraints on conduit size and processes, *J. Volcanol. Geotherm. Res.*, *178*, 10–18.

Nishida, K., H. Kawakatsu, Y. Fukao, and K. Obara (2008), Background love and Rayleigh waves simultaneously generated at the Pacific Ocean floors, *Geophys. Res. Lett.*, *35*, L16307, doi:10.1029/2008GL034753.

O'Brien, G. S., I. Lokmer, L. De Barros, C. J. Bean, G. Saccorotti, J.-P. Metaxian, and D. Patane (2011), Time reverse location of seismic long-period events recorded on Mt Etna, *Geophys. J. Int.*, *184*, 452–462.

Richardson, W. H. (1972), Bayesian-based iterative method of image restoration, *J. Opt. Soc. Am.*, *62*(1), 55–59.

Trabant, C., A. R. Hutko, M. Bahavar, R. Karstens, T. Ahern, and R. Aster (2012), Data products at the IRIS DMC: Stepping stones for research and other applications, *Seismol. Res. Lett.*, *83*(6), 846–854.

Walker, K. T., and P. M. Shearer (2009), Illuminating the near-sonic rupture velocities of the intracontinental Kokoxili M_w 7.8 and Denali fault M_w 7.9 strike-slip earthquakes with global P wave back projection imaging, *J. Geophys. Res.*, *114*, B02304, doi:10.1029/2008JB005738.

Zhang, H., R. M. Nadeau, and M. N. Toksoz (2010), Locating nonvolcanic tremors beneath the San Andreas Fault using a station-pair double-difference location method, *Geophys. Res. Lett.*, *37*, L13304, doi:10.1029/2010GL043577.